

Shock Capturing for Supersonic Flows Using a Pressure-Based Algorithm With a Semi-Retarded Density

G. Zhou, L. Davidson and E. Olsson

Thermo- and Fluid Dynamics, Chalmers University of Technology,
S-412 96 Gothenburg, Sweden

An improved pressure-based finite volume approach for solving Euler/Navier-Stokes equations is presented for calculating inviscid internal supersonic flow in a supersonic channel and external aerodynamic flow around the airfoil NACA 0012. This approach has previously shown a comparable ability of predicting inviscid transonic aerodynamic flow as density based methods and a better performance for turbulent flow. The aim of the present study is to investigate the oblique shock capturing properties of this method for fully supersonic flows. The new aspect of the work is to implement a semi-retarded density concept in an implicit numerical dissipation model to enhance the numerical stability in supersonic flows. The results for shocked supersonic channel are presented and compared with analytical ones. The computations for airfoil flow with strong shocks are also performed and presented. The second-order upwinding scheme which is used for the supersonic free stream flow around the airfoil, is shown to give a better resolution of the tail oblique shocks. The computational results for the test cases show that the presented algorithm achieves a quite satisfactory ability of oblique shock capturing.

1 Introduction

The pressure based method has been improved in many aspects. The most interesting issue is that the pressure based method have been successfully extended to carry out transonic aerodynamic flow simulations (Refs. 1, 2, 3). Traditionally, most transonic aerodynamic flow simulations were worked out with density based (or time-marching) methods in which density is used as a primary variable in the continuity equation. The efforts in Refs. 1, 2, 3 have shown that an advanced pressure based method can achieve a comparable accuracy to time-marching methods for inviscid flows. For turbulent transonic flows it has been shown that the pressure-based approach has a better performance. In this paper, interest is focused on the oblique shock capturing performance of the method with an inviscid supersonic free stream condition.

It is well-known that any type of scheme requires a proper artificial dissipation model. Much effort has been made to minimize artificial dissipation while still achieving numerical stability. Both the density based methods and the pressure-based method needs a dissipation model which combines the fourth-order and the second-order differencing terms of certain variables. The difference is that density based method use the dependent variables (Refs. 4, 5, 6), and the pressure-based method uses pressure for all equations. In this

latter method the fourth-order terms of the numerical dissipation model are attributable to use of a momentum interpolation like the Rhie-Chow interpolation (Ref. 7), which decouples the interpolation of the momentum from the interpolation of the driving force like pressure gradient and buoyancy. The second-order terms are attributable to use of the semi-retarded density which is used for decoupling of velocity from the mass flux. For transonic flow, the traditional retarded density introduces enough artificial dissipation to dampen the destabilizing effect without smearing the physical discontinuity at shocks. In this paper we show that the traditional retarded density is not suitable for full supersonic flow with strong shocks. A semi-retarded density is proposed to enhance the stability in these cases.

Two case are chosen to test the shock capturing properties of the method. One is supersonic channel flow with oblique incidence and reflected shocks. It is a part of a supersonic wedge cascade (Refs. 8, 9). This design gives a good test case for oblique shock capturing properties. The results are compared with the analytical solution. The second test case is supersonic flow around airfoil NACA 0012. This case involves a bow shock and a pair of oblique tail shocks.

2 Governing Equations

The inviscid flow is governed by Euler equations which can be obtained setting viscous terms equal to zero in Navier-Stokes equations. The integral form of Euler equations for an arbitrary stationary control volume δv with boundary $\delta\Omega$, and outer normal unit vector \mathbf{n} at surface element ds , in a Cartesian reference frame, can be written as

$$\int_{\delta v} \frac{\partial \Phi}{\partial t} dv + \int_{\delta\Omega} \mathbf{F} \bullet \mathbf{n} ds = \int_{\delta v} S_{\Phi} dv \quad (1)$$

where

$$\Phi = \begin{bmatrix} \rho \\ \rho \mathbf{V} \\ E \end{bmatrix}, \mathbf{F} = \begin{bmatrix} \rho \mathbf{V} \\ \mathbf{V} \Phi \\ H \mathbf{V} \end{bmatrix}, S_{\Phi} = \begin{bmatrix} 0 \\ -\nabla P \\ 0 \end{bmatrix}$$

Here Φ is the vector of the dependent variables, \mathbf{F} is the flux tensor, S_{Φ} is the source term, ρ and P are the fluid density and pressure. $\mathbf{V} = [U, V]^T$, where U and V are the velocity components in the x and y directions respectively. The equations (1) must be solved in conjunction with the perfect gas relationships

$$\begin{aligned} H &= C_p T + 0.5 |\mathbf{V}|^2 \\ P &= \rho R T. \end{aligned}$$

To avoid solving the energy equation, we adopt the assumption of constant enthalpy $H = H_0$. In the present scheme the continuity equation is transformed into a pressure correction equation by using truncated momentum equations.

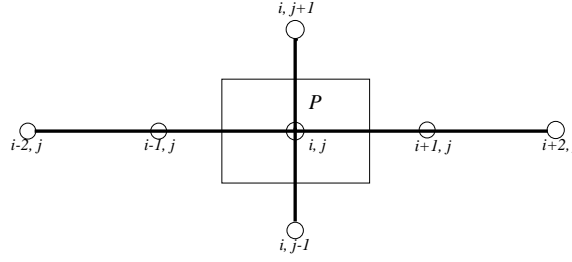


Figure 1. The control volume.

After the pressure correction is obtained, the pressure and mass flux component Φ are updated using the pressure correction. Then the density ρ can be related to pressure by the equation

$$\rho = \frac{\gamma P}{(\gamma - 1) (H_0 - 0.5|\mathbf{V}|^2)}. \quad (2)$$

where γ is the specific heats.

3 Numerical Approach

3.1 Cell-Centred Finite Volume Scheme

The physical domain is divided into quadrilateral control volumes, see Fig. 1. Note that we use cell-centred stationary grids. All the geometrical properties of the transformation from physical domain to computational domain are calculated and stored at the cell center (Ref. 10).

By assuming that all properties in the center are averaged over each cell and separating the space and time discretization, we can get the discretized equation as

$$(\Phi - \Phi^0) \frac{\delta v}{\Delta t} + \sum_{m=1}^4 (\mathbf{F} \bullet \mathbf{A}) + DP = S_\Phi \delta v \quad (3)$$

where Φ^0 is the value at previous time level, m each face \mathbf{A} of the control volume. DP is artificial dissipation terms. For uniform grid and two-dimensional flow it can be explicitly written as

$$DP = D_x P + D_y P \quad (4)$$

where $D_x P$ and $D_y P$ are the contributions for the two coordinate directions, respectively, which have the form (for $U_\eta, U_\xi > 0$):

$$\begin{aligned} D_x P &= \left\{ d_{i+1/2,j} - d_{i-1/2,j} \right\}; \\ D_y P &= \left\{ d_{i,j+1/2} - d_{i,j-1/2} \right\}. \end{aligned} \quad (5)$$

The d 's in the above equation can be written

$$\begin{aligned} d_{i+1/2,j} &= A_x \mu_{i+1/2} \left(P_{i+1/2,j} - P_{i-1/2,j} \right) \\ &+ B_x (P_{i+2,j} - 3P_{i+1,j} + 3P_{i,j} - P_{i-1,j}) \end{aligned} \quad (6)$$

where A and B are coefficients imposed by momentum and state equations. Smoothing function μ is obtained from a semi-retarded density concept

$$\bar{\rho} = \rho - \mu \frac{\Delta x}{2} \rho_x. \quad (7)$$

The difference from the traditional retarded density methods is that we use half central differencing (Semi-retarded) rather than back differencing. Here ρ_x is central differencing of the density. It can be shown that this semi-retarded density is equivalent to the first-order upwinding density used in Refs. (11, 12). The smoothing function adjusts the amount of second order dissipation by a two-level filters (for details see Refs. 2, 3).

Since the flux $(\mathbf{F} \bullet \mathbf{A})$ is expressed at cell surface m , proper discretization schemes should be used to evaluate cell face values of dependent variables. A wide variety of schemes have been implemented, e.g. first-order upwind, hybrid (Ref. 15), second-order upwind (Ref. 16), MUSCL (Ref. 18), third-order QUICK (Ref. 17), and CHARM (Ref. 20). Since the inherent dissipation in each scheme is different, it requires a flexibility of implementation of the numerical dissipation model. The previous investigations have shown that the proposed numerical method can easily meet this requirement.

The time dependent terms in present algorithm are treated in an *implicit* fashion, practical time steps are set to be

$$\Delta t = K[\min(\Delta t_\xi, \Delta t_\eta)]$$

where

$$\Delta t_\xi = \frac{\Delta \xi}{|\mathbf{V} \cdot \hat{\xi}|}, \quad \Delta t_\eta = \frac{\Delta \eta}{|\mathbf{V} \cdot \hat{\eta}|}$$

and K can be larger than unity.

The final discretized equation can be written in the standard form as

$$a_P \Phi_P = \sum a_{nb} \Phi_{nb} + S_C^\Phi \quad (8)$$

where subscript nb denotes neighbour and

$$a_P = \sum a_{nb} - S_P^\Phi.$$

The coefficients a_{nb} contain contributions from convection. S_C^Φ contains the source terms due to the pressure derivative and $\delta v / \Delta t \Phi^0$, and S_P^Φ contains the remaining terms. It should be mentioned that when Eq. (3) is cast into the form of the Eq.(8), additional source terms must be considered due to the choice of dependent variables as mass flux components.

Convection does not include density in this variable option, which gives a *convecting source term*. This can be expressed as

$$(S_P^\Phi)_{add1} = \sum_m \left[\frac{(\rho \mathbf{V}) \cdot \mathbf{A}}{\bar{\rho}} \right]_m.$$

It should be pointed out that in order to balance the discretized equation, the semi-retarded density $\bar{\rho}$ should be used in the term $(S_P^\Phi)_{add1}$.

3.2 Pressure Correction Equation

In this study, the mass flux components are selected as dependent variables instead of the velocities. This variable option allows for a direct relationship between momentum and pressure by truncating the momentum equations in the same way as in the conventional SIMPLE method (Ref. 15)

$$\mathbf{A} \cdot \Phi' = -\frac{\delta v}{a_P} \mathbf{A} \cdot \nabla P'. \quad (9)$$

It should be mentioned that in order to enhance stability of the original pressure correction equation, the density correction is carried out as (Ref. 19)

$$\rho' = \frac{\gamma P'}{(\gamma - 1) (H_0 - 0.5 |\mathbf{V}|^2)}. \quad (10)$$

Therefore, the discretized pressure correction equation becomes

$$\rho'_P \frac{\delta v}{\Delta t} + \sum_{m=1}^4 \left(\frac{\delta v}{a_P} \mathbf{A} \cdot \nabla P' \right) + \Delta \dot{m}_P = 0 \quad (11)$$

where $\Delta \dot{m}_P$ is the continuity error. This manipulation gives the pressure correction equation a hyperbolic appearance with respect to time.

The discretized equation for P' can also be cast into the form

$$a_P P'_P = \sum a_{nb} P'_{nb} + S_C \quad (12)$$

where S_C is mass residual.

3.3 Boundary Conditions

At a solid surface, a first-order extrapolation is used for both pressure and tangential component of velocity, i.e., assuming the second derivative in the normal direction to be zero. The density at the wall can then be extracted by enforcing constant free stream enthalpy at the wall.

Non-reflecting far field boundary condition (Ref. 5) is used for the airfoil flow. The boundary conditions are based on the theory of characteristics for locally one-dimensional inviscid flow. For supersonic inflow or outflow, the local one-dimensional Riemann invariants, entropy and tangential velocity component are given from outside or inside the computational region, respectively. These four quantities provide a complete definition of the flow at the far field boundary. A far field circulation correction is also used for the airfoil flow (Ref. 1, 2, 4, 5).

For the internal supersonic channel case presented, obviously all the variables are prescribed at the inlet, and all variables are extrapolated at outlet.

The boundary conditions for the pressure correction P' , either at the wall or at far field boundaries, are obtained using first-order extrapolation.

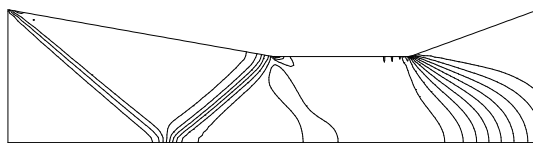


Figure 2. Pressure contours for supersonic channel $M_{inlet} = 2.0$

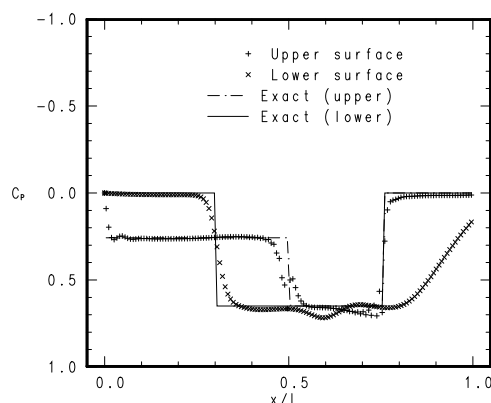


Figure 3. Surface pressure distribution $M_{inlet} = 2.0$

4 Results and Discussion

In this paper the main emphasis is concentrated on the implementation of an improved pressure based method in fully supersonic internal/external flow cases. For supersonic free stream flow cases, it was found that the traditional retarded density was not capable of damping the numerical instability. Therefore, a new semi-retarded density concept is designed to introduce second-order dissipation for both supersonic channel and airfoil flows.

I. Supersonic Channel Flow

A supersonic channel, which is a part of the supersonic wedge cascade designed by Denton (Ref. 8), is chosen as a test case for oblique shock capturing. In this channel, the leading edge shock, with inlet Mach number 2.0, is reflected from the lower surface and canceled out exactly at the corner of the upper surface. This condition then gives a uniform flow between the parallel surface and an expansion off the downstream corner. Grid distribution for this case is 138×36 . First-order upwind scheme was used. The computed results are shown in Fig. 2 and Fig. 3. The main interest of this work is the prediction of two oblique shocks and expansion waves. As shown in Fig. 2, a sharp leading edge shock is captured, while the reflected shock is smeared in several lines. Due to this finite thickness, the reflected shock is consequently not completely canceled out by the corner of the upper surface. Furthermore it causes oscillations in the parallel region as shown in Fig. 3. Comparing our results and those of Refs. 8 and 9 show that the solution of the present method has a more uniform region after the reflected shock.

II. Airfoil Flow

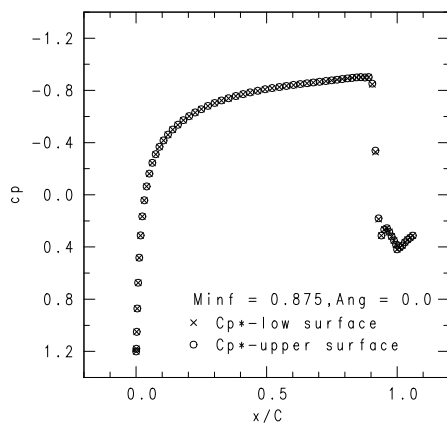
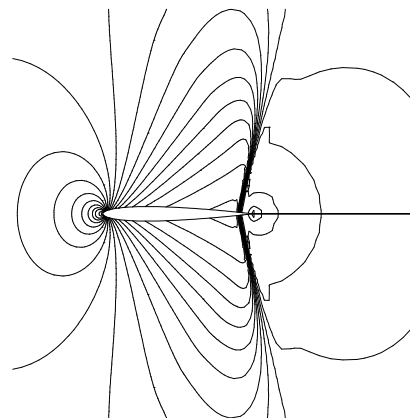


Figure 4a. Pressure coefficients,



4b. Pressure contours.

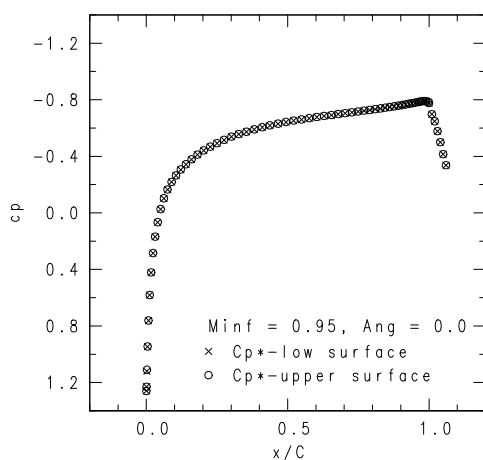
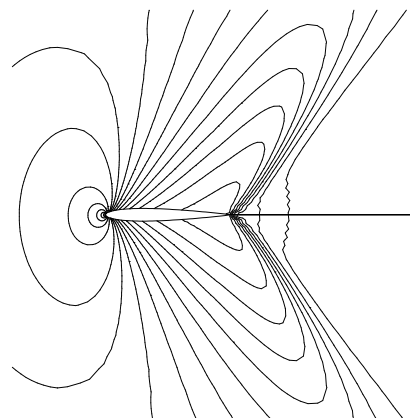


Figure 5a. Pressure coefficients,



5b. Pressure contours.

The proposed pressure based method has been applied to many transonic airfoil flow cases, which include both inviscid and turbulent flow simulations of NACA 0012 and RAE 2822. It was found that the use of retarded density, which introduce second-order dissipation in the supersonic region, was sufficient to achieve a converging solution of any subsonic free-stream cases. Figs. 4, 5 show computed results for free stream Mach number $M_\infty = 0.875$ and $M_\infty = 0.95$ respectively. Two sharp shocks appear on the airfoil surface in Fig. 5, smearing only in 3 cells. It is believed that the smearing is due to the requirement of cells involved in numerical differencing scheme. The results indicates that the numerical dissipation method with retarded density gives

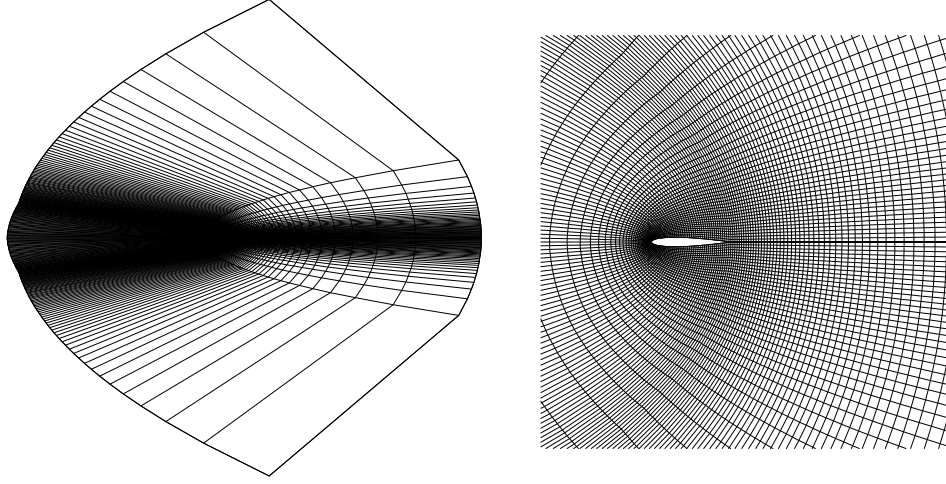


Figure 6a. Global view of grids, 6b. Enlargement in vicinity of surface

just enough dissipation keeping stability without heavy smearing physical discontinuities for transonic flows.

The grid used in present study for supersonic flow around NACA 0012 is a two-dimensional parabolic C-mesh, shown in Fig. 6. The far field boundaries of mesh are located approximately 40 chords upstream and downstream of the airfoil, and 47 chords laterally. The grid density is 250×78 . 100 nodes are located at the surface of the airfoil. The calculations are initialized with a uniform free stream flow at the prescribed Mach number and angle of attack. The convergence criterion is given as

$$|R|_2 = \left\{ \frac{1}{N} \sum_{i,j} (R_{i,j})^2 \right\}^{1/2}$$

where $R_{i,j}$ is the residual of continuity equation $|\Delta\rho/\Delta t|$ for cell (i, j) and N is the total number of control volumes. For a converged solution, the residual is reduced by 5 decades.

The predicted results of pressure distribution for cases $M_\infty = 1.20$, $\alpha = 0^\circ$ and $M_\infty = 1.20$, $\alpha = 7.0^\circ$, are presented in Figs. 7, 8. Both bow shock as well as typical fish tail shock are shown in Figs. 7. Note that the predicted bow shock is thicker than it should be. This is due to insufficient mesh resolution in this region. The sharp tail shocks are reasonably well captured in both cases. Fig. 7a shows the results obtained using first-order upwind scheme, while, Fig. 7b shows the results obtained using second-order upwind scheme. It is found that the second-order scheme shows higher resolution in the region near trailing edge. The weak normal shock in the fish tail intercepting the oblique shock is captured in this case. Furthermore, the oblique tail shock is sharper than that obtained using first-order upwind scheme. While the bow

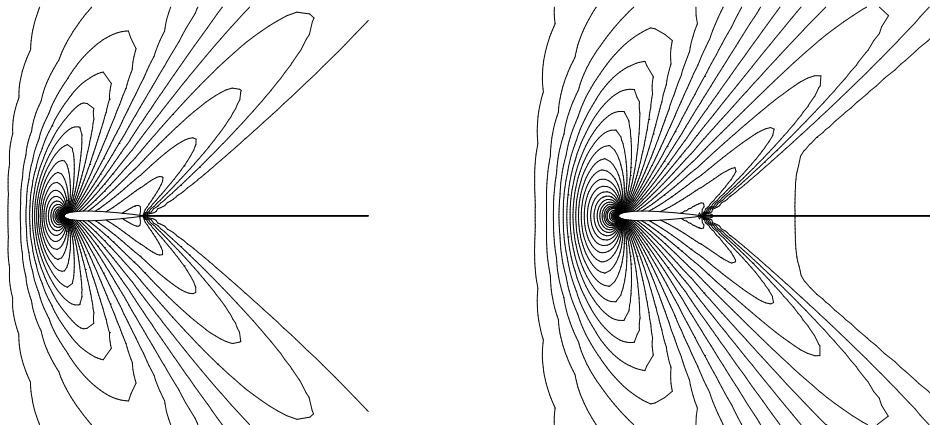


Figure 7a. First-order upwind scheme, 7b. Second-order upwind scheme, Pressure contours for $M_\infty = 1.2$, $\alpha = 0^\circ$

shock seems to move forward a little bit. Slight oscillations can be seen close the surface near trailing edge as shown in Fig. 7b.

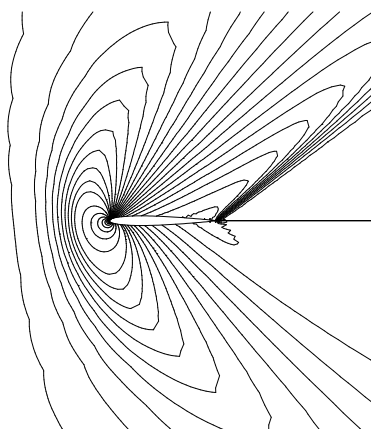


Figure 8. Pressure contours for $M_\infty = 1.2$, $\alpha = 7.0^\circ$, MUSCL scheme.

Fig. 8 presents the results using second-order MUSCL scheme for $\alpha = 7^\circ$. Some oscillations can also be noticed in the converged solution near trailing edge. It indicates that higher order scheme gives rise to less dissipation than lower order scheme, and that the damping mechanism involved in present algorithm is just enough to bound the destability.

5 Concluding Remarks

A cell-centred pressure based method for solving mass flux per unit area from Euler equations has been developed for calculating two-dimensional fully supersonic flows in both a channel and around an airfoil. A semi-retarded density method is used to contribute the second-order dissipation in the fully supersonic region to achieve the stability. For the internal supersonic flow the first-order upwind scheme is used. For the airfoil flow, both first-order and the second-order upwind scheme is used. The results demonstrates that the hybridization of the semi-retarded density and second-order schemes is capable of successful simulation of fully supersonic airfoil flow for the presented cases. No other special method for convergence acceleration has been introduced except for local varying time steps. Future research efforts are concentrated on the acceleration of convergency and advanced turbulence modeling.

References

1. Lai, Y. G., So, R. M. C. and Przekwas, A. J. – Aerodynamic Flow Simulation Using a Pressure-Based Method and a Two Equation Turbulent Model, AIAA paper 93-2902, July, (1993).
2. Zhou, G. and Davidson, L. – A Pressure Based Euler Scheme for Transonic Internal and External Flow Simulation, *Int. Journal CFD*, vol, 5, No. 1-2, (1995).
3. Zhou, G., Davidson, L. and Olsson, E. – Turbulent Transonic Airfoil Flow Simulation Using a Pressure-Based Algorithm, *AIAA Journal* , Vol. 33, No. 1, 42-47 (1995).
4. Jameson, A., Schmidt, W. and Turkel, E. – Numerical Solutions of the Euler Equations by Finite Volume Methods Using Runge-Kutta Time-Stepping Schemes, AIAA paper 81-1259, June, (1981).
5. Rizzi, A. – Spurious Entropy and Very Accurate Solutions to the Euler Equations, AIAA Paper 84-1644, June, (1984).
6. Pulliam, T. H. and Barton, J. T., – Euler Computations of AGARD Working Group 07 Airfoil Test Cases, AIAA paper 85-0018, January, (1985).
7. Rhie, C. M. and Chow, W. L.,– Numerical Study of the Turbulent Flow Past an Airfoil with Trailing Edge Separation, *AIAA Journal*, Vol. 21, 1527-1532 (1984).
8. Denton, J. D. – An Improved Time-Marching Method for Turbomachinery Flow Calculation, *Trans. ASME*, vol. 105, 514-524 (1983).
9. Liu, F. and Jameson, A. – Cascade Flow Calculations by a Multigrid Euler Method, *J. Prop. Power* Vol. 9, No. 1, 90-97 (1993).

10. Davidson, L. and Farhanieh, B., – A Finite-Volume Code Employing Collocated Variable Arrangement and Cartesian Velocity Components for Computation of Fluid Flow and Heat Transfer in Complex Three-Dimensional Geometries, Rept. 92/4, Thermo and Fluid Dynamics, Chalmers University of Technology, Gothenburg, (1992).
11. Wornom, S. F. and Hafez, M., – Calculation of Quasi-one-dimensional Flows With Shocks, *Computers and Fluids*, Vol. 14, No. 2, 131-140 (1986).
12. Lien, F-S and Leschziner, M. A., – Approximation of Turbulence Convection in Complex Flows with A TVD-MUSCL Scheme, *Proc. 5th Int. IAHR Symp. on Refined Flow Modeling and Turbulence Measurements*, 183-190, Paris, Sept. (1993).
13. Karki, K. C. and Patankar, S. V., – Pressure Based Calculation Procedure for Viscous Flows at All Speeds in Arbitrary Configurations, *AIAA Journal*, Vol. 27, 1167-1174 (1989).
14. Zhou, G. and Davidson, L., – Transonic Flow Computation Using a Modified SIMPLE Code Based on Collocated Grid Arrangement, *Proc. First European CFD Conference*, Brussels, Vol. 2, 749-756 (1992).
15. Patankar, S. V., – *Numerical Heat Transfer and Fluid Flow*, McGraw -Hill, Washington (1980)
16. Shyy, W. and Chen, M. H., – Pressure-Based Multigrid Algorithm for Flow at All Speeds, *AIAA Journal*, Vol. 30, 2660-2669 (1992).
17. Leonard, B. P., – A Stable and Accurate Convective Modelling Procedure Based on Quadratic Upstream Interpolation, *Computer Methods in Applied Mechanics and Engineering*, Vol. 19, 59-97 (1979).
18. van Leer, B., – Towards the Ultimate Conservation Difference Scheme V, A Second-order Sequel to Godunov's Method, *Journal of Computational Physics*, Vol. 32, 101-129 (1979).
19. Mcguirk, J. J. and Page, G. J., – Shock Capturing Using a Pressure-Correction Method, *AIAA Journal*, Vol, 28, No. 10, 1751-1757 (1990)
20. G. Zhou, and L. Davidson and E. Olsson, – Transonic Inviscid/Turbulent Airfoil Flow Simulations Using a Pressure Based Method with High Order Schemes, *Proceeding of the 14th International Conference on Numerical Method in Fluid Dynamics*, (eds. S. M. Deshpande, S. S. Desai, R. Narasimha), 372-377, Springer-Verlag. Berlin, 1995.